Octa-band reconfigurable monopole antenna frequency diversity 5G wireless

Ali Kadhum Abd, Jamal Mohammed Rasool
Department of Communication Engineering, Faculty of Engineering, University of Technology- Iraq, Baghdad, Iraq

Article Info

ABSTRACT

An octa-band frequency-reconfigurable antenna ($28\times14\times1.5$ mm^3) with a broad tuning range is shown. Antenna mode1 (4.31 GHz) works in one single-band mode and two dual-band in modes 2 and 3 (i.e., 3.91 and 5.9 GHz) as well as one tri-band in mode 4 (i.e., 3.09, 5.65, and 7.92 GHz) based on the switching situation of the antenna. Changing capacitance for frequency reconfigurability is accomplished with the use of lumped components. The antenna's observed tuning spans from 3.09 GHz to 7.92 GHz. for all the resonant bands, the suggested antenna has a voltage standing waves ratio (VSWR)<1.45 except for one band with a VSWR<1.85. From 70.57% to 97.93%, the suggested structure's radiation efficiency may be calculated. For a better understanding proposed antenna's far field and scattering characteristics, we used CST Microwave Studio 2021. We may conclude that our suggested antenna is suitable for today's wireless applications, which need multiband and multimode small antennas. Using a small stainless-steel wire as a switch, a prototype of the antenna design is built and tested to verify the simulation findings. The suggested reconfigurable antenna's strong concordance between simulated and measured findings.
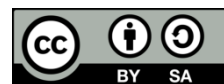
Corresponding Author:

Ali Kadhum Abd
College of Communication Engineering, University of Technology- Iraq
Baghdad, Iraq
Email: coe.20.06@grad.uotechnology.edu.iq

1. INTRODUCTION

Faster and more reliable mobile communications are the goals of fifth generation (5G) technology, which operates in the sub-6 GHz frequency band. Conventional antennas can no longer serve wireless communication systems that need several wireless services in a single device. An antenna that can adapt to the application is created to meet those needs. An antenna that can be reconfigured is known as a reconfigurable antenna [1]. Antennas that can be changed according to frequency, pattern, or polarization are known as reconfigurable. With a specific frequency range. It is feasible to utilize the whole spectrum of frequencies using reconfigurable antennas, which can be adjusted to any required band of frequencies [2]. Pattern reconfigurable antennas may be used to guide mobile network beams in the future by changing their emission pattern in a specific direction. With multiple input, multiple output (MIMO) services, antennas that can change their pattern and beamwidth are also a feasible alternative [3]. Improve reception efficiency and reduce co-channel interference using antennas with reversible polarization [4]. Several switching techniques may be used to reconfigure the antenna [5]. It is worth noting that reconfigurable antennas have several advantages over multiband antennas in pre-filtering and reducing complexity. Positive-intrinsic-negative (PIN) diodes, micro-mechanical systems (MEMS) switches, and varactors may be used in the antenna body to allow frequency adjustment. By changing the antenna's effective length, you can change

the antenna's operating frequency [6]. Antennas that can be reconfigured at various frequencies are reported in the literature. A three-pin diode frequency reconfigurable monopole antenna is described in [7]. These diodes changed the antenna's effective length to alter the resonance frequency. A reconfigurable frequency antenna (F-shape antenna) capable of hopping between six frequencies was created in [8]. An RF-4 substrate, two PIN diodes, and a truncated ground plane are used to build the antenna. This antenna was large and had a high-order harmonic component, both of which could be seen in the reflection coefficient plots for each switch mode [9]. The reconfigurable Wi-Fi, wireless local-area network (WLAN), and worldwide interoperability for microwave access (WiMAX) antennas were developed with the multiband antenna as the foundation. Even though it is tiny, it cannot cover the whole 5 GHz band in a single mode. To support multi-radio wireless systems, they demonstrated a reconfigurable monopole antenna. All four bands are reporting good antenna performance. The antenna's huge size necessitates using a filter to block specific frequencies. WiMAX's monopole antenna is now available in a dual-band configuration in versions [10], [11]. A varactor diode was used to modify the frequency range of the antenna. Nonetheless, its efficiency is low, and its advantages are seen throughout a large country [12]. These two monopole antennas have been proposed for WiMAX and WLAN. These antennas have a small size and excellent performance. Copper tape and gab replicate a diode's ON and OFF states, allowing the authors to customize their device.

This work develops a compact, octa-band frequency reconfigurable monopole antenna on a 1.5 mm thick FR-4 substrate with a new form and design. The monopole antenna can transmit data in eight distinct frequencies; In addition to the 5G cellular spectrum, the suggested antenna covers WLAN and WiMAX. The lumped element's RLC (inductance, resistance, and capacitance) components are employed as switches inside frequency reconfigurability via simulating the antenna's radiating structure. For integration, each switch has its own 1 mm slot. However, the behavior of PIN diodes like switch ON-OFF is utilized in the measurement to achieve frequency reconfigurability. The rest of the paper is organized: the theory, geometry, and switching mechanisms of the innovative octa-band antenna are covered in section 2. Section 3 covers the simulated and measured situations as well as the outcomes. Section 4 finishes the paper.

2.   PROPOSED ANTENNA DESIGN

Octa-band frequency reconfigurable monopole antenna fundamental geometry, design theory, and switching approaches are discussed in this part. The antenna design was reworked to function in a single band, two dual-band modes, and a single tri-band mode using lumped element switches in the modeling environment. It is possible to reconfigure the circuit using PIN diodes in the measurement setup. Using metallic ground planes with shortened lengths may achieve greater efficiency and excellent far-field radiation patterns.

2.1. Structural geometry

Antenna for WiMAX, 5G, WLAN, Wi-Fi, applications for fixed mobile communication (FMC) and radio altimeter in octa-band frequency reconfigurable form is illustrated in Figure 1. The antenna's radiating element is printed on the FR-4 substrate and adhered to a metallic ground surface that has been blunted (with a tangent loss (tan) of 0.02). As the FR-4 substrate is widely available, designing an antenna is more affordable and feasible. The best gain, efficiency, and directivity may be obtained by using truncated metallic ground surfaces in combination with A stub that provides for post-fabrication tuning for more efficient impedance matching with the truncated and above it on the back. The antenna is excited via a 50-ohm microstrip line of 2.8 mm wide. We utilize the waveguide port designated for the feed line to excite it. Lumped element switches may be included in the radiating structure via three slots with a 1 mm width, as illustrated in Figure 1. To put it simply: the dimensions of this suggested antenna are 28×14×1.5 mm.

2.2. Study parameter

In the process of designing the antenna, we went through several steps to reach the final shape, and we used a study of the parameter in the CST Microwave Studio to get the final form of the antenna that works according to the required frequencies. At each stage, we improve performance by adding a patch with the diode that we represented in the form of resistance in this antenna. Do some enhancement of the parameter like (Lf+L2) for mode 1 and W2 for mode 2 and L4 for mode 3 and W5 for mode 4. The best parameters for (Lf+L2), W2, L4, and W5 are 19, 4, 7, and 2.25 mm; respectively, they are chosen by the best S11 with suitable frequency. Figure 2 shows that operation. The suggested structure's precise dimensions are shown in Table 1.
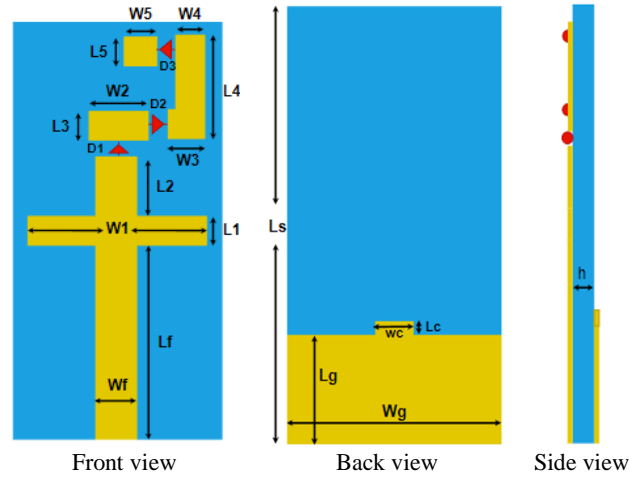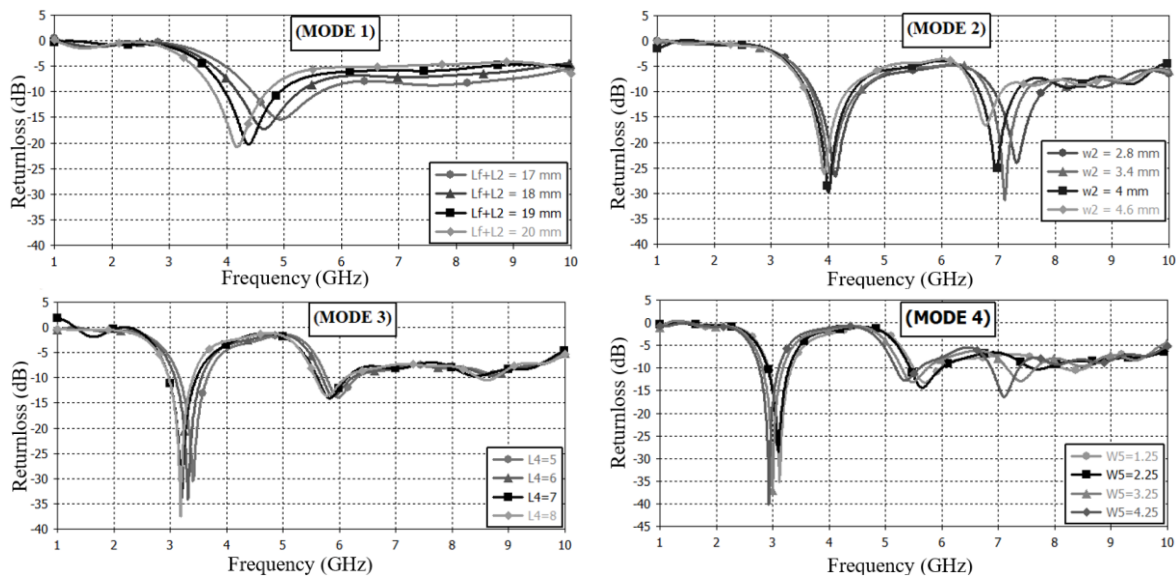
Figure 1. The proposed antenna's geometry

Figure 2. The study parameter for mode 1, mode 2, mode 3, and mode 4

Table 1. Planned antenna's dimensions

Parameters	Value (mm)	Parameters	Value (mm)
Ls	28	L5	2
Wg	14	Wf	2.8
Lg	7	Wc	2.5
Lf	13	W1	12
Lc	1	W2	2.5
L1	2	W3	3.995
L2	4	W4	2
L3	2	W5	2.25
L4	7	h	1.5

2.3. The theoretical basis for the antenna's layout

To accommodate the switches, 1 mm slots have been carved into the radiating patch at suitable places. The transmission line model theory is used to estimate the antenna's resonant lengths [13]. By applying the law from (1) to (10) to find Lf that represents, in this case, $L_{4.31}$, $L_{3.91}$, $L_{6.95}$, $L_{3.2}$, $L_{5.9}$, $L_{3.06}$, $L_{5.65}$, and $L_{7.92}$ To get the desired frequency modes, the switching states must be adjusted. As an example, let us use the guided wavelength and resonant length as (1) to (10).

$$L_{4.31} = \lambda_{4.31}/4 \tag{1}$$

$$L_{3.91} = \lambda_{3.91}/4 \tag{2}$$

$$L_{6.95} = \lambda_{6.95}/4 \tag{3}$$

$$L_{3.2} = \lambda_{3.2}/4 \tag{4}$$

$$L_{5.9} = \lambda_{5.9}/4 \tag{5}$$

$$L_{3.06} = \lambda_{3.06}/4 \tag{6}$$

$$L_{5.65} = \lambda_{5.65}/4 \tag{7}$$

$$L_{7.92} = \lambda_{7.92}/4 \tag{8}$$

$$\varepsilon_{eff} = \frac{\varepsilon_r+1}{2} + \frac{\varepsilon_r-1}{2}\left(1 + 12\left(\frac{w}{h}\right)\right)^{-0.5} \tag{9}$$

$$Lf = \frac{Cv}{4f\sqrt{\varepsilon_{eff}}} \tag{10}$$

where cv represents the velocity of light in vacuum, ε_{eff} Effective dielectric constant, εr is the relative permittivity, h is the height or thickness, and w is the width of the substrate. Radiation efficiency may be determined using the equation in [14] to determine the guided wavelength and antenna quality. The efficiency increases, and the reflection coefficient decreases when the antenna is stimulated in the correct location. Which can be expressed by the rule as:

$$|\Gamma| = \frac{Z_0 - Z_1}{Z_0 + Z_1}$$

where Z_1 is the antenna characteristic impedance and Z_0 is the feed line characteristic impedance, voltage standing waves ratio (VSWR), and the reflection coefficient (S11) of an antenna are linked. It is said that VSWR can be defined as:

$$vswR = \frac{1 + |\Gamma|}{1 - |\Gamma|}$$

the reflection coefficient (S11<-10 dB) in the target frequency range is lower when the antenna is completely matched. When designing a radio antenna's radiation efficiency, it is essential to consider its directivity (D) and gain (G). When describing gain, it is customary to use decibels (dB) and can be provided:

$$G(dB) = 10 \times log_{10}(\eta radD)$$

2.4. Switching techniques

Because of their high radio frequency (RF) functioning, PIN diodes serve as variable resistors in RF circuits. Figure 3 shows the switch configuration. On the other hand, PIN diodes have more sophisticated circuitry for the ON and OFF states as shown in Figure 3(a). Inductance (L) is present in the ON and OFF states of similar PIN diodes. For the ON state, it is simply an RL series circuit, with a low-value resistor (RL) and an inductor (L). An inductor (L) coupled in series with a high-value resistor (Rh) and a capacitor (C) is identical to an RLC circuit in the OFF state. Figure 3(b) demonstrates that the PIN diodes are formed as two RLC boundary conditions fused together.

The recommended antenna's reconfigurable properties have been recreated using simple resistors. Using the RLC lumped model and PIN diode model, we did not include capacitance and inductance values in the simulation since the switch ON state in both of these models aids the flow of currents on the radiating route of the structure. Because of this, both types of open-circuit termination occur when the power is turned OFF. For both the ON and OFF states of PIN diodes, an analogous circuit model was previously developed [15]. PIN diode literature reveals that a series RL component with very small values serves as an open circuit to enable current to travel down the radiator. While this is true for most diodes, the OFF state of a PIN diode can only be described as a parallel RLC component with values so that current cannot flow with the radiator.

An RLC lumped element model with fundamental resistor values has been employed to construct the switch in our model to simplify the open circuit and short circuit behavior. A resistor (RL) with a small value of 4.586×10^{-8} Ω that value comes from (11) in [16] because its use in the proposed antenna rope wire stainless steel similar cylinder with length (2 mm) and radius (0. 1 mm) behaves as a short circuit and allows the normal current flow can calculate that resistant by (12) in [17] Figure 4. Displays A constructed model of the suggested antenna, built on the FR-4 substrate with a thickness of 1.5 mm and a relative permittivity *εr=4.3*. For actual operations, the antenna is supplied via an SMA connector. Use rope length of 2 mm, and a radius of 0.1 mm like switches to accomplish the multiple modes of operation in the antenna. On the other hand, a resistance (Rh) of 1 MΩ has exhibited open-circuit behavior and blocks the path for the current to flow along with the radiating structure.

$$A = \pi r^2 \tag{11}$$

where A is cross-sectional area of cylinder and r is the radius of the circular disk in meter.

$$\rho = \frac{RA}{L} \tag{12}$$

where, ρ is resistivity (Ω•m) at 20 °C, R is resistance Ω for the matching in antenna, L is length of wire rope ρ for stainless steel=72×10^{-8}, and A=$3.14 \times (0.1)^2 = 0.0314$.

$$R = \frac{\rho L}{A} = \frac{72 \ x \ 10^{-8} x \ 2 \ x \ 10^{-3}}{0.0314} = 4.586 \times 10^{-8}$$
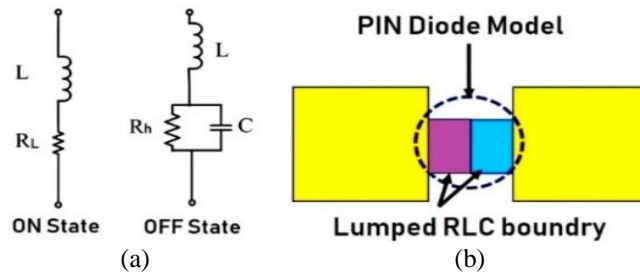

Figure 3. Switch configuration (a) for ON and OFF states of operation on diode model and (b) the model in CST
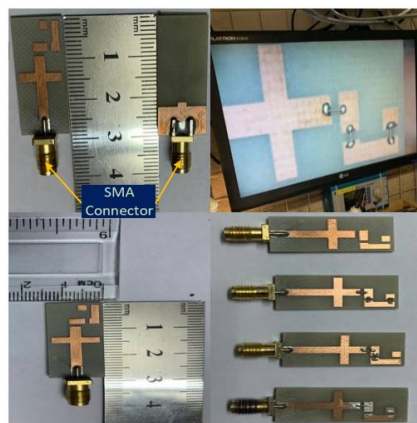

Figure 4. The fabricated prototype for the octa-band antenna

This indicates the effective resonant lengths at the respective frequencies in the whole patch, demonstrating the inverse relationship with the frequency; as shown in Table 2, the lumped element switch is used; therefore, it can be represented in CST as a resistor. of 4.586×10^{-8} Ω for ON mode and 1 MΩ for OFF

mode, to represent. The reconfigurable monopole antenna's reflection coefficient (S11) is tested using Agilent Technologies E5071C 30 kHz- 20GHz, as shown in Figure 5.

Table 2. The octa-band antenna's tuning states

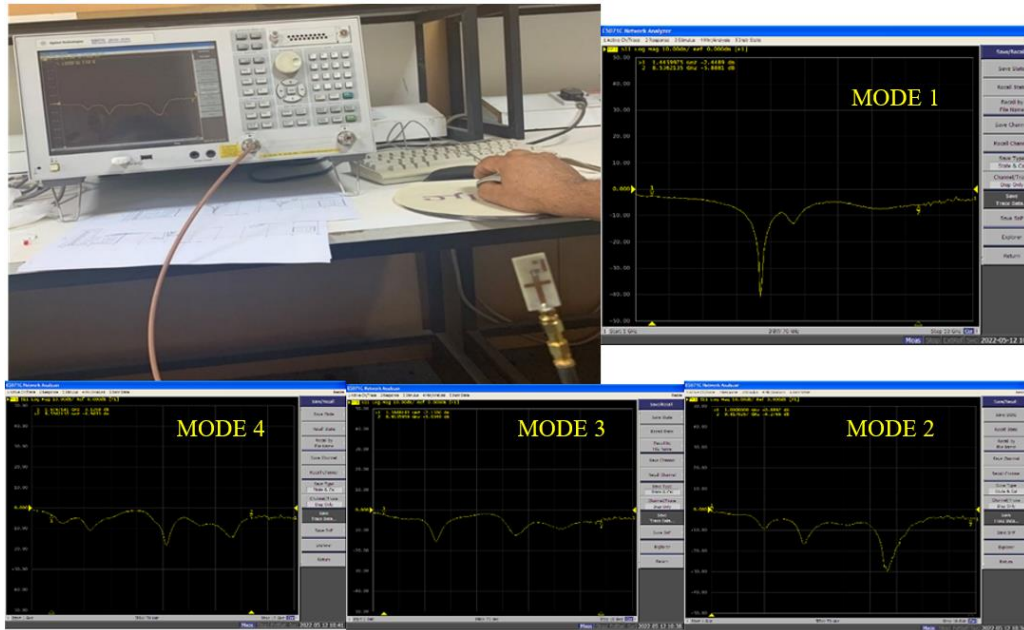| Modes	D1	D2	D3	Resonant Bands (GHz)
1	OFF	OFF	OFF	4.31
2	ON	OFF	OFF	3.91 and 6.95
3	ON	ON	OFF	3.2 and 5.9
4	ON	ON	ON	3.06, 5.65 and 7.92

Figure 5. The measuring set-up used to determine the reflection coefficient of (S11) using Agilent Technologies E5071C

3. RESULTS AND DISCUSSION

CST Microwave Studio (MWS) 2021 was used to build, model, and analyze the radiating structure in order to assess the octa-band antenna's performance. A waveguide port is used to power the proposed antenna. The CST MWS 2021 transient solver analyzes VSWR, directivity, gain, far-field pattern, surface current distribution, and reflection coefficient under open-add-space boundary conditions.

3.1. Return loss and bandwidth

In mode 1, As soon as all of the switches have been, the proposed antenna operates in single band mode at 4.31 GHz with a return loss of -58.39 dB when switched OFF and a simulated bandwidth of 1150 MHz (3.86 to 5.01 GHz). In mode 2, Only one of the three switches (D1) is ON; the other two are OFF; the antenna operates in a dual-band mode at 3.91 and 6.95 GHz with a return loss of -30.23, -23 dB, and bandwidth of 810 MHz (3.58 to 4.39 GHz) and 640 MHz (6.66 to 7.30 GHz), respectively. In mode three, in dual-band mode, two switches (D1 and D2) are turned ON, while one switch (D3) is turned OFF, i.e., 3.2 and 5.9 GHz, with a return loss of -26.81 and -17.82 dB and bandwidth of 480 MHz (2.98 to 3.46 GHz) and 660 MHz (5.61 to 6.27 GHz), respectively. In mode 4, Switches 1 and 2 and 3 are turned ON simultaneously, and the antenna performs optimally. The return loss at 3.06, 5.65, and 7.92 GHz is -22.74, -14.76, and -10.52 dB, and bandwidths of 420 MHz (3.28 to 2.86 GHz), 560 MHz (5.42 to 5.98 GHz), and 350 MHz (7.7 to 8.05 GHz) respectively. Figures 6(a) to 6(d) depict the monopole octa-band antenna's measured and simulated reflection coefficients.

It is worth noting that the measured and simulated findings are in good agreement. The planned antenna has a VSWR of less than 1.45 for all the frequency bands except one band with a VSWR of less than 1.85 to ensure the antenna's match is perfect. VSWR at 3.06, 3.2, 3.91, 4.31, 5.65, 5.9, 6.95, and 7.92 GHz is 1.15, 1.09, 1.06, 1.00, 1.44, 1.29, 1.15, and 1.84, respectively, as illustrated in Figure 7.
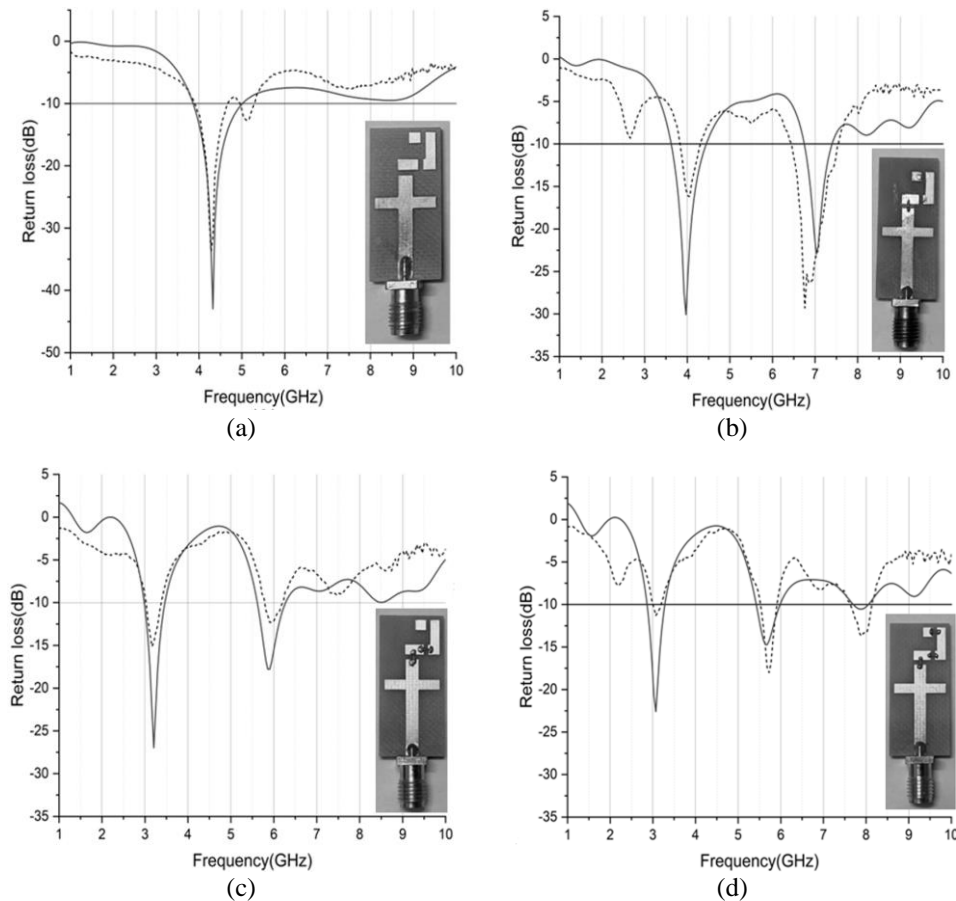
Figure 6. The simulated and measured return loss occurs in all operational modes (a) mode 1 4.31 GHz,
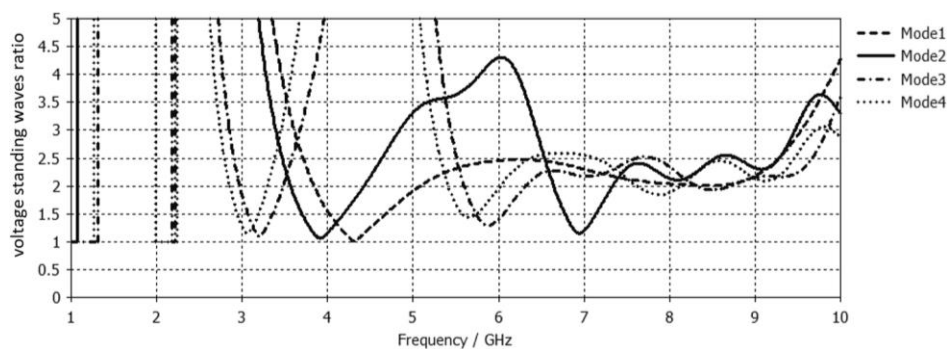(b) mode 2 3.91 and 6.95 GHz, (c) mode 3 3.2 and 5.9 GHz, and (d) mode 4 3.06,5.65 and 7.92 GHz

Figure 7. Voltage standing waves ratio (VSWR) of the proposed antenna in different operating modes

3.2. Far field radiation pattern

The proposed antenna for mode 1 has a simulated peak gain and radiation efficiency of 2.51 dBi and
88.58%, respectively. They are operating at 4.31 GHz. At 3.91 and 6.95 GHz, mode 2 achieves a dual band
with a gain of 2.21 and 2.06 dBi and radiation efficiency of 97.93% and 70.57%, respectively. The antenna
operates at 3.2 and 5.9 GHz in mode 3, with peak gains of 1.78 and 1.93 dBi and radiation efficiencies of
96.04% and 80.75%, respectively. In mode 4, the proposed structure operates at 3.06, 5.165, and 7.92 GHz,
with peak gains of 1.59, 2.1, and 1.92 dBi and radiation efficiencies of 94.5%, 85.07%, and 70.76%,
respectively Figures 8(a) to 8(h), shows the simulated radiation pattern of the antenna in both the E-plane and
H-plane at the operating frequencies bands the shape of the radiation pattern in the E-plane resembles the
figure-of-eight at frequencies of 4.31, 3.91, 3.2, 3.06, and 5.65 GHz. In most frequency bands, the antenna's

radiation qualities in the H-plane are omni-directional. Resonant frequencies are shown in three-dimensional (3D) gain plots to understand better the antenna's radiation qualities in Figures 9(a) to 9(h).
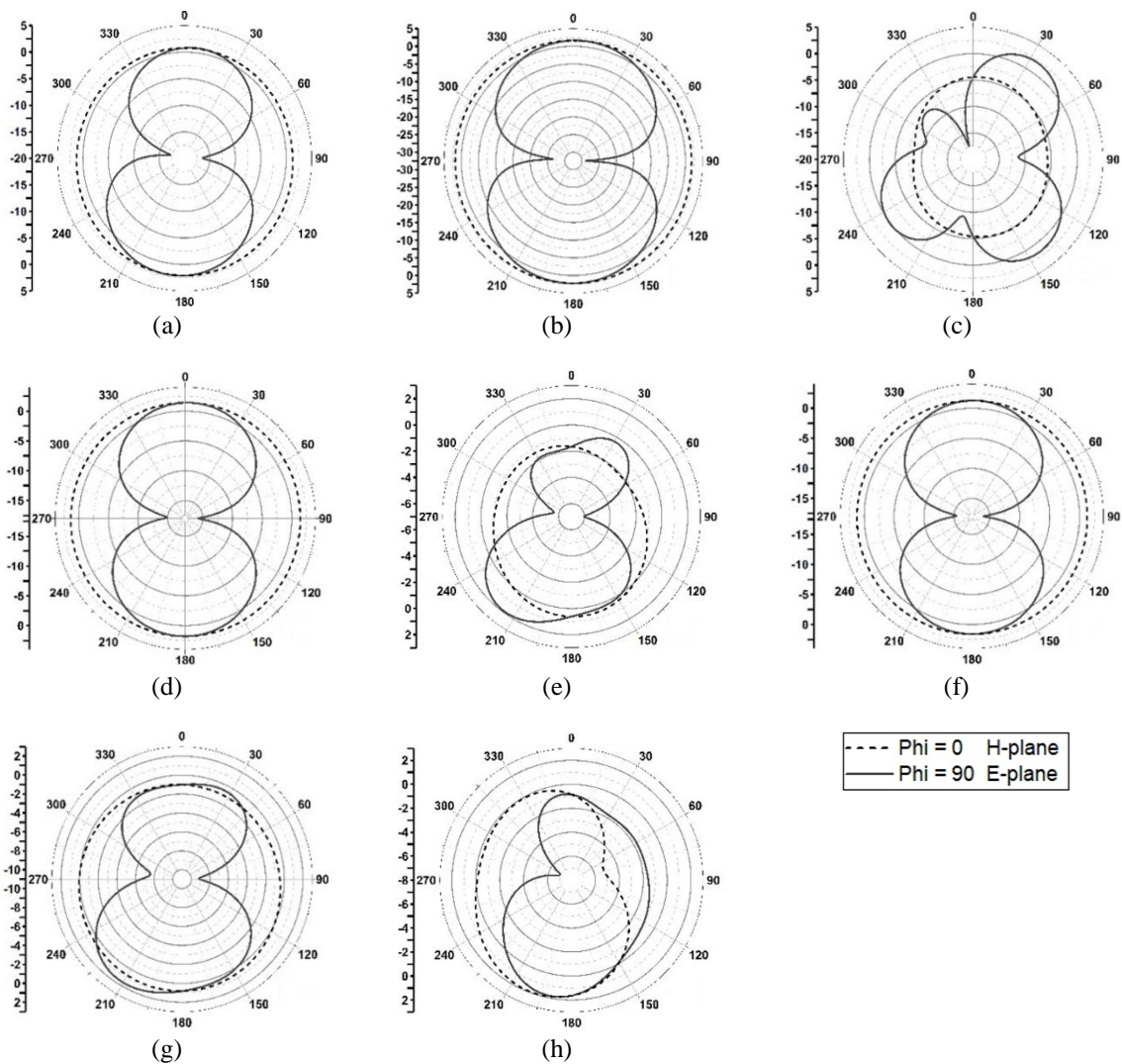

Figure 8. Simulation of the proposed antenna's radiation pattern at different frequencies and switching states (a) 4.31 GHz (mode 1), (b) 3.91 GHz (mode 2), (c) 6.95 GHz (mode 2), (d) 3.2 GHz (mode 3), (e) 5.9 GHz (mode 3), (f) 3.06 GHz (mode 4), (g) 5.65 GHz (mode 4), and (h) 7.92 GHz (mode 4)

3.3. Surface currents

As shown in Figures 10(a) and 10(b) the surface currents may be seen when an antenna operates in various modes of operation. It is possible to use the antenna at a 4.31 GHz frequency, and the density of the surface currents contributes to radiation at that frequency. Dual-band operation is possible in modes 2 and 3 (i.e., 3.91 and 6.95 GHz, 3.2 and 5.9 GHz). Radiator surface currents show that lower bands are dominated by a bigger fraction, whereas the higher bands are dominated by a smaller section of the radiator. There is a three-band (i.e., 3.06 to 5.65 and 7.92 GHz) mode 4 operation. There is a larger surface current density over the radiator's length, which suggests that the whole metallic radiator is contributing to lower frequency radiation (i.e., 3.06 GHz). It is worth noting that the radiator's top bands are being radiated by smaller sections (5.65 and 7.92 GHz). As the resonant frequency rises, the length of the resonant frequency decreases, thereby confirming the inverse connection between frequency and resonant length. The performance matrices of the suggested antennas are summarized in Table 3. We can determine their lengths using (13) [16]. The current distribution's outcomes are exactly what we predicted. It is possible that the calculated lengths (optimal lengths) change somewhat from the simulation because of differing radiator widths, diodes, and biasing effects.

$$L_{monopole} = \frac{3\times10^8}{4\times f_r \times 2\sqrt{\frac{\varepsilon_r+1}{2}+\frac{\varepsilon_r-1}{2}(1+12(\frac{h}{W}))^{-0.5}}} \tag{13}$$

where f_r is the frequency desired, ε_r is relative permittivity of the substrate, h is high substrate and w is width of radiation element.
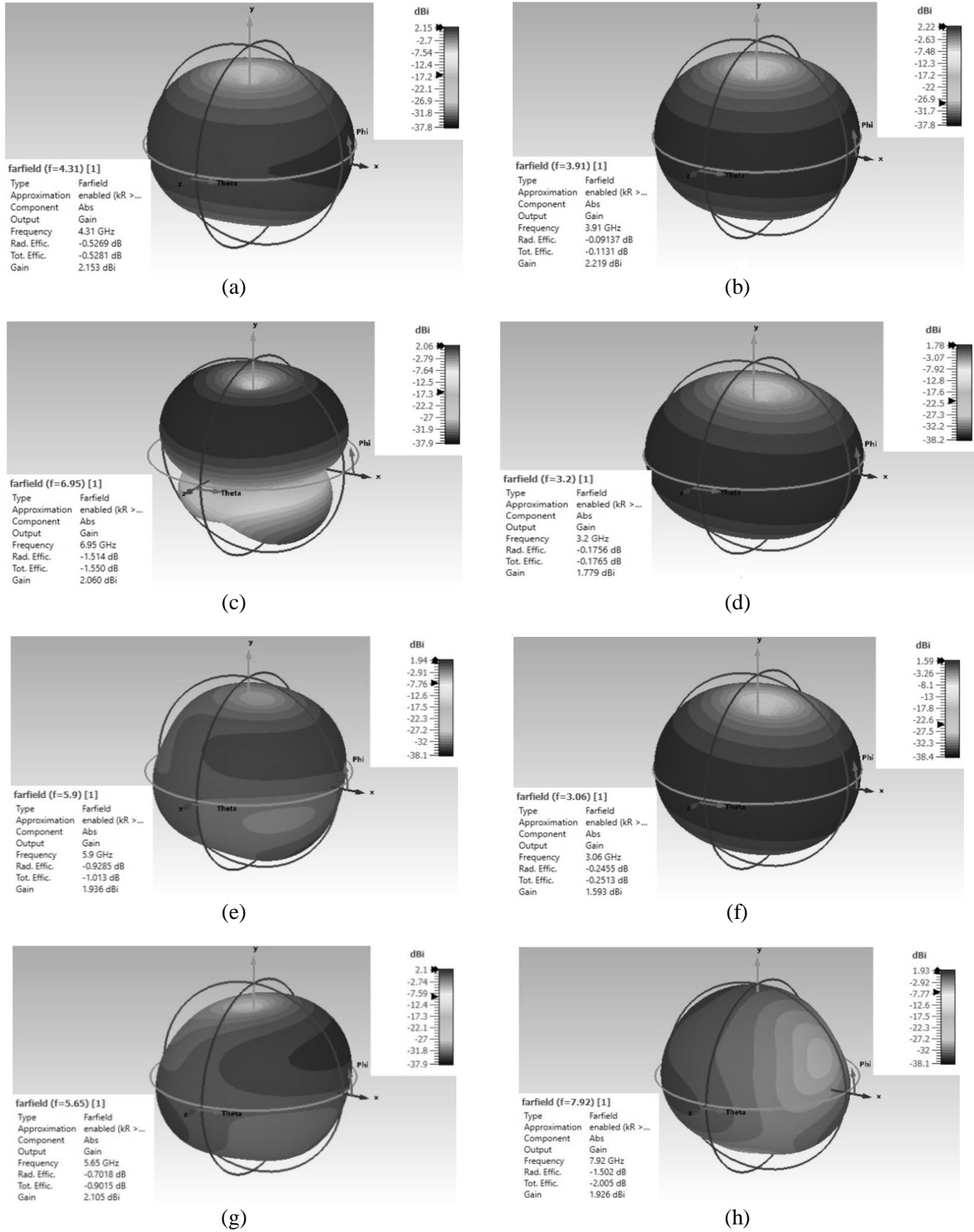

Figure 9. The 3D gain pattern plots at (a) 4.43 GHz (mode 1), (b) 3.5 GHz (mode 2), (c) 5.66 GHz (mode 2), (d) 3.1 GHz (mode 3), (e) 5.5 GHz (mode 3), (f) 2.9 GHz (mode 4), (g) 5.14 GHz (mode 4), and (h) 5.7 GHz (mode 4)
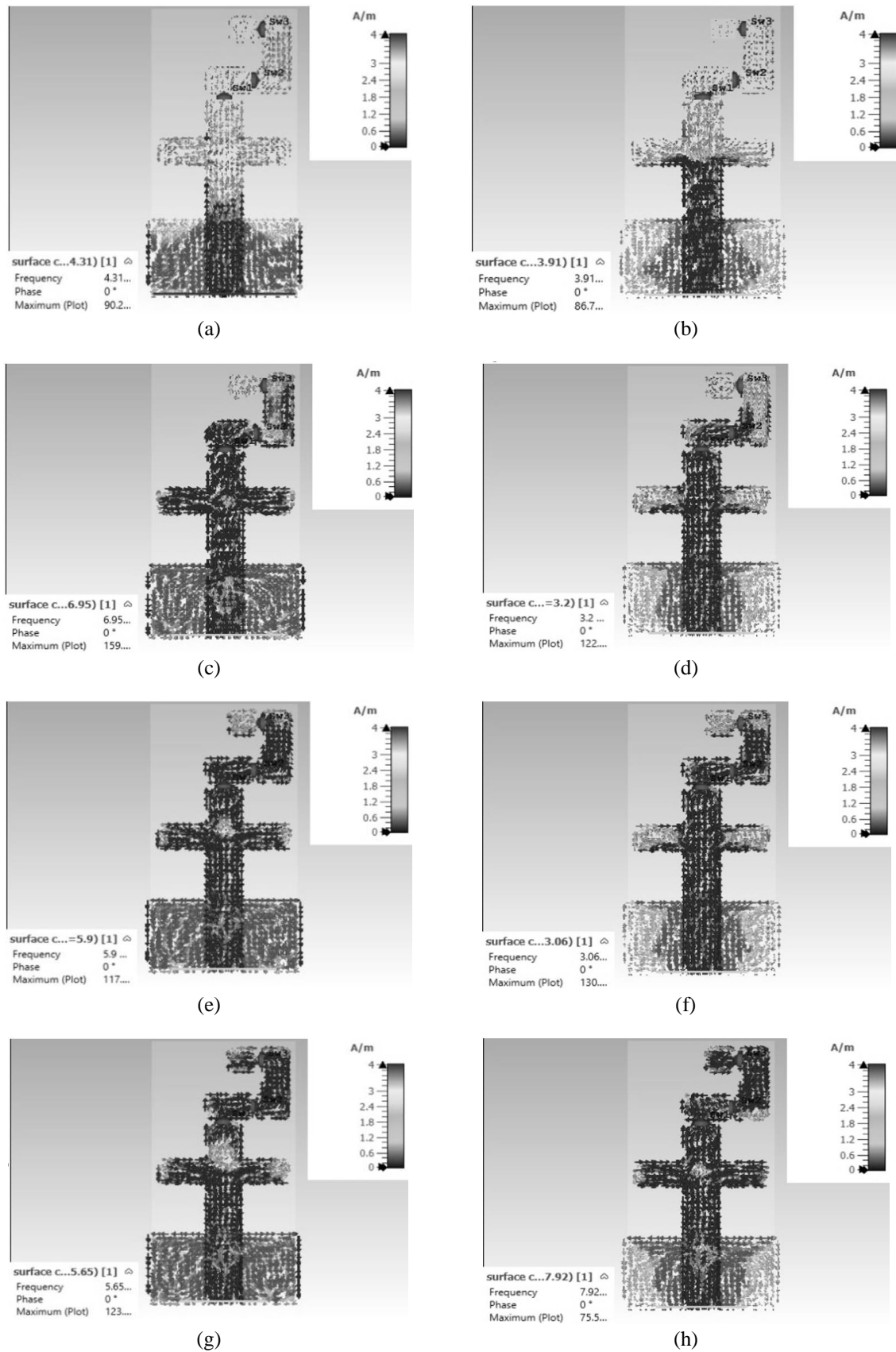
Figure 10. The proposed antenna's surface current in various modes (a) 4.31 GHz (mode 1), (b) 3.91 GHz (mode 2), (c) 6.95 GHz (mode 2), (d) 3.2 GHz (mode 3), (e) 5.9 GHz (mode 3), (f) 3.06 GHz (mode 4) (continue), (g) 5.65 GHz (mode 4), and (h) 7.92 GHz (mode 4)

The suggested antenna is more compact than the antennas described in [18]–[26] in terms of dimensions. With a 350 to 1150 MHz bandwidth, the proposed antenna has more bandwidth than antennas constructed in [20], [23], also higher gain than [23], and has a higher radiation efficiency than antennas designed in [18]–[26]. Compared to other potential antennas, the most notable difference is that the suggested antenna can function over eight different frequency bands, which is more than any other antenna has been able to do and has a higher radiation efficiency. The comparison is shown in Table 4.

Table 3. The antenna's results

Parameters	D (1, 2, 3) OFF mode1	D (1 ON and 2, 3 OFF) mode2		D (1, 2 ON and 3 OFF) mode3		D (1, 2, 3) ON mode4		
Frequencies (GHz)	4.31	3.91	6.95	3.2	5.9	3.06	5.65	7.92
Gain (dBi)	2.15	2.21	2.06	1.78	1.93	1.59	2.1	1.92
Return loss (dB)	-58.39	-30.23	-23	-26.81	-17.82	-22.74	-14.76	-10.52
Directivity (dBi)	2.67	2.31	3.57	1.95	2.86	1.83	2.8	3.42
VSWR	1	1.06	1.15	1.09	1.29	1.15	1.44	1.84
Bandwidth %	26.68	20.71	9.2	15	11.18	13.72	9.91	4.41
Efficiencies %	88.58	97.93	70.57	96.04	80.75	94.5	85.07	70.76

Table 4. A comparison of the proposed antenna to previously reported works

Ref. no.	Dimension (mm)	Total no of operating Bands	Operating frequencies (GHz)	Bandwidth (MHz)	Peak gains (dBi)	Radiation efficiency (%)
[18]	53×35	3	2.45, 3.5, 5.2	319 to 947	1.92 to 3.01	85 to 90
[19]	40×35	3	2.45, 3.5, 5.4	490 to 1360	1.92 to 3.02	76.4 to 86.5
[20]	60×60	5	2.4, 4.26, 4.32, 4.58, 5.76	60 to 170	1.31 to 2.77	-
[21]	33.5×16	2	2.4, 5	250 to 1450	1.5 to 3.5	80 to 95
[22]	39×37	3	2.4, 3, 5.4	550 to 1220	1.27 to 3.8	>90
[23]	37×35	4	2, 3.4, 2.4, 3.1	200 to 960	1.76 to 1.98	>85
[24]	53×35	3	2.45, 3.5, 5.2	330 to 1250	1.48 to 3.26	84.6 to 92.5
[25]	40×35	6	2.10, 2.40, 3.35, 3.50, 5.28, 5.97	335 to 1220	1.92 to 3.8	92.5 to 97
[26]	40×22	4	2.45, 5.13, 3.49, 5.81	750 to 1260	1.72 to 2.96	76.4 to 92
This work	28×14	8	3.06, 3.2, 3.91, 4.31, 5.65, 5.9, 6.95, 7.92	350 to 1150	1.59 to 2.21	70.57 to 97.93

4. CONCLUSION

As part of this study, we created and experimentally tested a new octa-band frequency reconfigurable monopole antenna design. Reconfiguration of the monopole's antenna allowed it to be used in various modes. As a result of the different switching states, the necessary performance characteristics were achieved. The requisite performance characteristics were achieved by the use of several switching states. Antenna coverage is limited to a single frequency when all switches are OFF (4.31 GHz). Dual bands of 3.2 and 5.9 GHz are possible when D1 is activated. During dual-band operation, the prototype is activated by turning ON both D1 and D2 (3.2 and 5.9 GHz). When all switches are switched ON, the antenna may simultaneously function at three different frequencies (3.06, 5.65, and 7.92 GHz). In addition to its compact size, low cost, and lightweight, the proposed antenna has a wide range of applications, including GSM, UMTS, 4G-LTE, WiMAX, and WLAN Wireless networks as fixed satellite services in the 6 GHz frequency band. The antenna also supports the sub-6GHz 5G bands of 3.06, 3.2, 3.91, and 4.31 GHz. the suggested antenna's measurements and simulations agreed rather well.

REFERENCES

[1] M. K. Shereen, M. I. Khattak, and G. Witjaksono, "A brief review of frequency, radiation pattern, polarization, and compound reconfigurable antennas for 5G applications," *Journal of Computational Electronics*, vol. 18, no. 3, pp. 1065–1102, Sep. 2019, doi: 10.1007/s10825-019-01336-0.

[2] J. Costantine, Y. Tawk, S. E. Barbin, and C. G. Christodoulou, "Reconfigurable antennas: design and applications," *Proceedings of the IEEE*, vol. 103, no. 3, pp. 424–437, 2015.

[3] I. F. Akyildiz, W.-Y. Lee, M. C. Vuran, and S. Mohanty, "NeXt generation/dynamic spectrum access/cognitive radio wireless networks: A survey," *Computer Networks*, vol. 50, no. 13, pp. 2127–2159, Sep. 2006, doi: 10.1016/j.comnet.2006.05.001.

[4] S. Nikolaou *et al.*, "Pattern and frequency reconfigurable annular slot antenna using PIN diodes," *IEEE Transactions on Antennas and Propagation*, vol. 54, no. 2, pp. 439–448, Feb. 2006, doi: 10.1109/TAP.2005.863398.

[5] B. Kim, B. Pan, S. Nikolaou, Y.-S. Kim, J. Papapolymerou, and M. M. Tentzeris, "A novel single-feed circular microstrip antenna with reconfigurable polarization capability," *IEEE Transactions on Antennas and Propagation*, vol. 56, no. 3, pp. 630–638, Mar. 2008, doi: 10.1109/TAP.2008.916894.

[6] M. N. Osman, M. K. A. Rahim, P. Gardner, M. R. Hamid, M. F. M. Yusoff, and H. A. Majid, "An electronically reconfigurable patch antenna design for polarization diversity with fixed resonant frequency," *Radioengineering*, vol. 24, no. 1, pp. 45–53, Apr. 2015, doi: 10.13164/re.2015.0045.

[7] J. M. Rasool, "A proposed ultra-wideband antenna for 5G communications using frequency band expanding," *International Journal of Computing and Network Technology*, vol. 7, no. 1, pp. 2–5, Jan. 2019, doi: 10.12785/ijcnt/070101.

[8]   J. M. Rasool, "A proposed design of unit cell of metamaterial for 5G mobile communication," *Telecommunication Computing Electronics and Control (TELKOMNIKA)*, vol. 15, no. 3, Sep. 2017, doi: 10.12928/telkomnika.v15i3.6079.

[9]   I. A. Shah *et al.*, "Design and analysis of a hexa-band frequency reconfigurable antenna for wireless communication," *AEU-International Journal of Electronics and Communications*, vol. 98, pp. 80–88, Jan. 2019, doi: 10.1016/j.aeue.2018.10.012.

[10]   M. M. Al-Saeedi, A. A. Hashim, O. Al-Bayati, A. S. Rasheed, and R. H. Finjan, "Design of dual band slotted reconfigurable antenna using electronic switching circuit," *Indonesian Journal of Electrical Engineering and Computer Science (IJEECS)*, vol. 24, no. 1, pp. 386–393, Oct. 2021, doi: 10.11591/ijeecs.v24.i1.pp386-393.

[11]   A. Iqbal and O. A. Saraereh, "A compact frequency reconfigurable monopole antenna for WI-FI/WLAN applications," *Progress in Electromagnetics Research Letters*, vol. 68, pp. 79–84, 2017, doi: 10.2528/PIERL17041203.

[12]   S. Sharma and C. C. Tripathi, "Wideband to concurrent tri-band frequency reconfigurable microstrip patch antenna for wireless communication," *International Journal of Microwave and Wireless Technologies*, vol. 9, no. 4, pp. 915–922, May 2017, doi: 10.1017/S1759078716000763.

[13]   F. Hirtenfelder, "Effective antenna simulations using CST Microwave Studio," in *2007 2nd International ITG Conference on Antennas*, Mar. 2007, p. 239, doi: 10.1109/INICA.2007.4353972.

[14]   A. Pandey, "Practical microstrip and printed antenna design," Artech House, 2019, pp. 1–6.

[15]   S. V Rakibe, S. D. Sahu, and S. V Khobragade, "Fractal antenna for multi-frequency applications using PIN diode," *Journal of Computational Electronics*, vol. 14, no. 1, pp. 222–226, Mar. 2015, doi: 10.1007/s10825-014-0640-6.

[16]   C. A. Balanis, *Antenna theory: analysis and design*. John Wiley and Sons, 2016.

[17]   W. M. Haynes, "CRC handbook of chemistry and physics," *Journal of the American Pharmaceutical Association*, pp. 3–488, 1942.

[18]   S. Ullah, S. Hayat, A. Umar, U. Ali, F. A. Tahir, and J. A. Flint, "Design, fabrication and measurement of triple band frequency reconfigurable antennas for portable wireless communications," *AEU-International Journal of Electronics and Communications*, vol. 81, pp. 236–242, Nov. 2017, doi: 10.1016/j.aeue.2017.07.028.

[19]   S. A. A. Shah, M. F. Khan, S. Ullah, and J. A. Flint, "Design of a multi-band frequency reconfigurable planar monopole antenna using truncated ground plane for Wi-Fi, WLAN and WiMAX applications," in *2014 International Conference on Open Source Systems and Technologies*, Dec. 2014, pp. 151–155, doi: 10.1109/ICOSST.2014.7029336.

[20]   B. Saikia, P. Dutta, and K. Borah, "Design of a frequency reconfigurable microstrip patch antenna for multiband applications," *SSRN Electronic Journal*, pp. 8–11, 2020, doi: 10.2139/ssrn.3516619.

[21]   A. I. AL-Muttairy and M. J. Farhan, "Frequency reconfigurable monopole antenna with harmonic suppression for IoT applications," *Telecommunication Computing Electronics and Control (TELKOMNIKA)*, vol. 18, no. 1, Feb. 2020, doi: 10.12928/telkomnika.v18i1.12699.

[22]   A. Iqbal, S. Ullah, U. Naeem, A. Basir, and U. Ali, "Design, fabrication and measurement of a compact, frequency reconfigurable, modified T-shape planar antenna for portable applications," *Journal of Electrical Engineering and Technology*, vol. 12, no. 4, pp. 1611–1618, 2017, doi: 10.5370/JEET.2017.12.4.1611.

[23]   S. Ullah, I. Ahmad, Y. Raheem, S. Ullah, T. Ahmad, and U. Habib, "Hexagonal shaped CPW feed based frequency reconfigurable antenna for WLAN and sub-6 GHz 5G applications," in *2020 International Conference on Emerging Trends in Smart Technologies (ICETST)*, Mar. 2020, pp. 1–4, doi: 10.1109/ICETST49965.2020.9080688.

[24]   I. Ali Shah, S. Hayat, I. Khan, I. Alam, S. Ullah, and A. Afridi, "A compact, tri-band and 9-shape reconfigurable antenna for WiFi, WiMAX and WLAN applications," *International Journal of Wireless and Microwave Technologies*, vol. 6, no. 5, pp. 45–53, Sep. 2016, doi: 10.5815/ijwmt.2016.05.05.

[25]   S. Ullah, S. Ahmad, B. A. Khan, and J. A. Flint, "A multi-band switchable antenna for Wi-Fi, 3G Advanced, WiMAX, and WLAN wireless applications," *International Journal of Microwave and Wireless Technologies*, vol. 10, no. 8, pp. 991–997, Oct. 2018, doi: 10.1017/S1759078718000776.

[26]   S. A. A. Shah, M. F. Khan, S. Ullah, A. Basir, U. Ali, and U. Naeem, "Design and measurement of planar monopole antennas for multi-band wireless applications," *IETE Journal of Research*, vol. 63, no. 2, pp. 194–204, Mar. 2017, doi: 10.1080/03772063.2016.1261049.

BIOGRAPHIES OF AUTHORS

Ali Kadhum Abd received his B.E. degree in communication engineering from Iraq College in Basra in 2017. He is currently working on his M.Sc. degree in the Communication Engineering Department in the College of Engineering at the University of Technology, Baghdad, Iraq. Her research interests include IoT, antenna design, reconfigurable antenna design, and automation. He can be contacted at coe.20.06@grad.uotechnology.edu.iq.

Jamal Mohammed Rasool is an asst. professor in the Department of Communication Engineering University of Technology. He received his M.Sc. in electrical engineering from the University of Technology USSR/Odessa and his Ph.D. in communication (technical sciences) from the University of Technology Belarus/Minsk. He can be contacted at 30189@uotechnology.edu.iq.